Wave-Front Autoionization: Classical Decay of Two-Electron Atoms

Xiao Wang and W. E. Cooke
Department of Physics, University of Southern California, Los Angeles, California 90089-0484
(Received 11 April 1991)

When a rapidly decaying, autoionizing Rydberg series is excited with a short pulse, it may decay in a series of discrete "stair steps," separated in time by the classical Rydberg orbit period. A rapid core transition can generate a Rydberg shock front which itself produces stair-step changes in the core dipole moment each time the shock front passes. These core excitations significantly reduce the laser power and bandwidth requirements compared to those used in one-electron-like-atom wave-packet studies, while many of the same effects may be observed.

PACS numbers: 32.80.Rm, 32.80.Dz

A series of recent theoretical and experimental works have shown that one-electron atoms can be excited into wave-packet states, where the Rydberg electron behaves in a classical fashion, orbiting around the remaining ion with a period of $2\pi n^{*3}$ atomic units [1–3]. These wave packets are usually created by a short laser pulse which excites an electron into a coherent superposition of Rydberg states, and this packet is then detected by photoionizing with a second short laser pulse. The total production of ions is monitored as a function of the delay between the excitation and ionization pulses. Since the excitation and ionization processes occur primarily when the electron is near the ion, these processes are most efficient whenever the excitation and ionization pulses are separated by an integer number of Rydberg orbit periods. The number of detected ions thus oscillates up and down with increasing delay, just as the Rydberg electron oscillates around the ion. Henle, Ritsch, and Zoller have continued this approach with two-electron-like atoms, having the Rydberg wave packet scatter from the valence electron in the core [4].

However, Rydberg oscillations will usually persist for only a few periods, because the spacing between Rydberg states is not equal, as would be required for a coherent harmonic-oscillator state [5]. This makes the wave packet rather sensitive to the bandwidth of the exciting laser, and narrows the choices of principal quantum number appropriate for generating wave packets [6]. Even in the best of cases, the wave packet must eventually collapse, although one recent experiment has observed its revival [7]. In an earlier attempt to prevent this collapse, Stroud's group coherently excited a Stark manifold of states, where the states are more evenly spaced, and observed an *angular* wave packet [8].

Here, we demonstrate that a two-electron atom can show classical-like timing when one electron is excited to a Rydberg state, and the other is rapidly excited to a valence state. Autoionization, localized at the core, generates a sudden disturbance in the Rydberg wave function, which then propagates as a shock wave, moving at the classical orbit velocity. Each time the shock front passes the core, the core suffers a sudden change in its dipole moment. Thus, the dipole moment decays in a series of "stair steps," separated by the classical Rydberg orbit period. These autoionizing Rydberg states have the added advantages that the excitation and ionization processes are very efficient and that the atom itself filters the exciting laser so that the effect is relatively insensitive to the bandwidth and the tuning of the exciting laser. These advantages significantly reduce the requirements on the excitation laser power and bandwidth, so that these effects should be easily observable over a wider range of n values.

Over the last ten years, many autoionizing Rydberg states have been studied using the isolated core excitation (ICE) method [9], where a valence electron is first excited to a Rydberg state, and then a second "core" electron is excited. The second excitation is close to the *ionic* transition, while the Rydberg electron plays the role of a spectator. The only effects of the Rydberg electron are to broaden the ionic transition due to the autoionization process, and to introduce a small frequency shift, since the shielding interaction between the Rydberg and core electrons is slightly different when the core electron is excited. This change in the shielding also allows "shakeup" transitions to occur, where the Rydberg electron changes its principal quantum number [9–11].

For example, in barium, an ICE excitation might start from a $6s65g$ bound Rydberg state, which can be excited using standard techniques and long-pulse (5 ns) lasers [12]. Next, a short-pulse 455-nm laser would excite the $6s$ core electron to a $6p_{3/2}$ state:

$$6s65g+\hbar\omega\rightarrow 6p_{3/2}ng\,.$$

The transition moment for this excitation of the core electron has been shown to be well described [10,11] by the product of two factors:

$$T(W)\propto\frac{1}{\sin\pi(n^*+\delta+i\gamma/2)}\frac{\sin\pi(n^*-n_i^*)}{W_n-W_i}\,, \qquad (1)$$

where n^* represents the effective quantum number of the final $6p_{3/2}ng$ autoionizing state, δ is the quantum defect of the $6p_{3/2}ng$ series, γ is the scaled autoionization linewidth of the $6p_{3/2}ng$ series (the linewidth times n^{*3} is a constant for each state in the series), and n_i^* represents the effective quantum number of the initial bound state. The binding energy of a state, W, is related to the ef-

fective quantum number of the state by

$$W = -1/2n^{*2}. \quad (2)$$

Since autoionizing states decay so quickly, the uncertainty principle spreads the wave function over a large energy band, and the effective quantum number n^* becomes a continuous variable. This continuous n^* also represents the phase of the radial wave function in multichannel quantum-defect analyses [10]. The wave function is largest where $n^* + \delta$ is an integer, and the first factor in the transition moment of Eq. (1) is thus a resonant denominator which represents the amount of autoionizing-state character in an energy region. Each peak has a full width at half maximum of γ (for small γ) when plotted *versus* n^*. Since the energy spacing between Rydberg states is $1/n^{*3}$, a specific n state will have an autoionization rate of γ/n^{*3}. This n^* dependence can be eliminated by multiplying the rate times the classical Rydberg orbit period ($2\pi n^{*3}$), to identify $2\pi\gamma$ as the probability of autoionization per Rydberg orbit. This is the same for *all* n values, since autoionization only occurs when the Rydberg electron passes near the core electron, and this happens only once per orbit, regardless of the n state.

The second factor of Eq. (1) arises from the projection of the initial Rydberg wave function onto the final Rydberg wave function. The two wave functions see different core potentials, so they will generally have two different phase shifts arising from their core interactions. When the core is excited, the Rydberg electron must readjust, and consequently it can change its principal quantum number.

Consider the wave packet created when a short-pulse, broadband laser is used to excite the core. The time dependence of the wave packet can be determined by constructing the Fourier transform of the dipole moment:

$$\tilde{T}(t) = \int T(W) e^{iWt/\hbar} d(W/\hbar). \quad (3)$$

But the Fourier transform of this product transition moment is just the convolution of the Fourier transforms of each of the two factors. These two factors simplify considerably in the limit of large principal quantum numbers, where the energy spacing between Rydberg states is nearly constant, so that $\Delta E \approx \Delta n^*$. Then the first factor is similar to that for a Fabry-Pérot interferometer, so that the Fourierr transform represents a series of decreasing pulses, separated by the transit time for a single pass through the interferometer. The second factor is the Fourier transform of a square pulse. The convolution thus becomes a series of stair steps, which have an exponential envelope. This decay is a discretized version *in time* of the normal exponential decay. The dipole moment is constant for a Rydberg orbit period, and then decreases sharply to remain constant for yet another Rydberg orbit period.

Thus the square of the core dipole moment measures the flux of Rydberg-electron wave function incident on the core. After the initial excitation, a constant flux of electron enters and somewhat less leaves the core region, since autoionization reduces the outgoing bound flux. However, after a complete Rydberg orbit, the wave function then entering the core region has already passed through once, and so it must be reduced by the fraction $1 - e^{-2\pi\gamma}$. Thus, although the total autoionization may occur with a near-exponential decay, the wave-function density *near the core* changes classically, in discrete steps. The initial core excitation creates a *wave front* which originates at the core, travels out to the large-r region, and returns to the core in a classical Rydberg period. This heuristic understanding is remarkably robust, holding even when the principal quantum numbers are not very large, since the second factor in the transition moment strongly reduces the contributions from states much removed in energy.

Figure 1 illustrates these functions and their Fourier transforms in the limit of very large quantum numbers. Figure 1(a) shows the overlap function and the magnitude of its Fourier transform. Figure 1(b) shows the magnitude of the state density, and the magnitude of its Fourier transform. Figure 1(c) shows the product of the first two functions, and the magnitude of its Fourier transform.

When the quantum numbers are not extremely large, the unequal spacing between Rydberg states must be incorporated, and the transition moment must also be multiplied by the frequency spectrum of the exciting laser. Both of these factors have relatively minor effects, since the transition moment already restricts the bandwidth considerably. To illustrate this, we have used a Gaussian model for a Fourier-transform-limited laser pulse and Fourier transformed the product of this Gaussian fre-

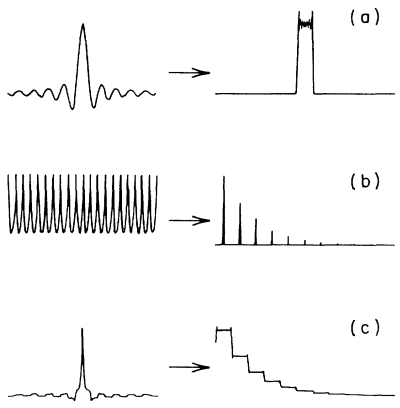

FIG. 1. Functions and their Fourier transforms in the limit of large principal quantum numbers: (a) the overlap function and the magnitude of its Fourier transform; (b) the magnitude of the state density, and the magnitude of its Fourier transform; (c) the product of the first two functions, and the magnitude of its Fourier transform.

quency spectrum and the transition moment of Eq. (1). Figure 2 shows the square of the Fourier transforms (power spectra) for three different laser pulse lengths (solid line, 1 ps; short-dashed line, 10 ps; and long-dashed line, 100 ps), for the transition $6s65g \rightarrow 6p_{3/2}ng$ in barium. In each of the figures, the zero of time has been chosen to be at the *peak* of the incident Gaussian laser pulse, so that the longer pulse begins considerably earlier than the short pulses. The $6p_{3/2}ng$ doubly excited states of barium [12] have quantum defects of approximately 0.015, and an autoionization probability per orbit of $2\pi\gamma \approx 0.31$, while the initial $6s65g$ Rydberg state [13] has a quantum defect of 0.047. With this choice of initial state, the classical Rydberg orbit period is 41 ps. Note that the finite laser bandwidth only causes major changes when the laser pulse length is longer than a Rydberg orbit so that the laser bandwidth becomes more restrictive than the transition moment. Otherwise, the finite laser bandwidth merely eliminates very high frequencies to smooth the time dependence of the dipole moment.

In these realistic profiles, two effects can be seen. The overall envelope is a series of stair-step decays as in the limiting case, and there is also clear evidence of the beating of waves, as in the one-electron-atom studies. The striking, nonexponential decay closely parallels the expected classical decay for an equivalent planetary system, where collisions between the two electrons could only occur at those times when the Rydberg electron passes the perihelion of its orbit. In the one-electron studies this decay is absent because the states live for many, many Rydberg orbit periods. Instead, the disappearance of the one-electron transition moment arises from a dephasing of the Rydberg states constructing the wave packet. Our profiles also show this dephasing; after several decay cycles, the interference between the various Rydberg states (which are not equally spaced) tends to wash out the steps, and the system returns to an exponential decay.

However, we can easily show the difference between the effects of dephasing of the dipole moment due to Rydberg wave interference from those of decay due to autoionization, by using an excitation laser which is tuned off resonance. In the wings, the overlap envelope $[\sin(\pi\Delta n^*)/\Delta W]$ has a much slower rate of change from one state to the next, so the excitation approaches that obtained in the one-electron studies. In Fig. 3, we show three time profiles, calculated using 10-ps laser pulses. The short-dashed line represents the dipole magnitude when the laser is on line center as in Fig. 2. The solid line represents the dipole magnitude enhanced by a factor of 14, when the laser is tuned five states to the red. The long-dashed line represents the dipole magnitude enhanced by a factor of 10, when the laser is tuned five states to the blue. Each of these detunings corresponds to approximately two laser linewidths. Note that the unequal spacing of Rydberg states is clearly discernible in the different frequency oscillations for the two detuned cases. For the excitations in the wings, the unbalanced frequency mix causes a rapid dephasing of the dipole moment so that it disappears much more rapidly. However, it reappears after a Rydberg orbit as the excited states beat. This reappearance is like the one-electron cases, since the square wave envelope has been effectively removed, and the positions and heights of these secondary peaks will strongly depend on the laser bandwidth and precise tuning.

The excitation in these transitions is not an excitation

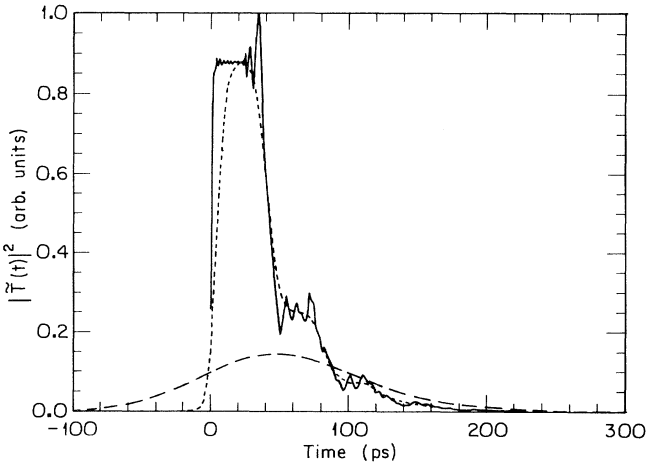

FIG. 2. The square of the Fourier transforms of the dipole moment for three different laser pulse lengths for the transition $6s65g \rightarrow 6p_{3/2}ng$ in barium. The solid line corresponds to 1 ps, the short-dashed line corresponds to 10 ps, and the long-dashed line corresponds to 100 ps.

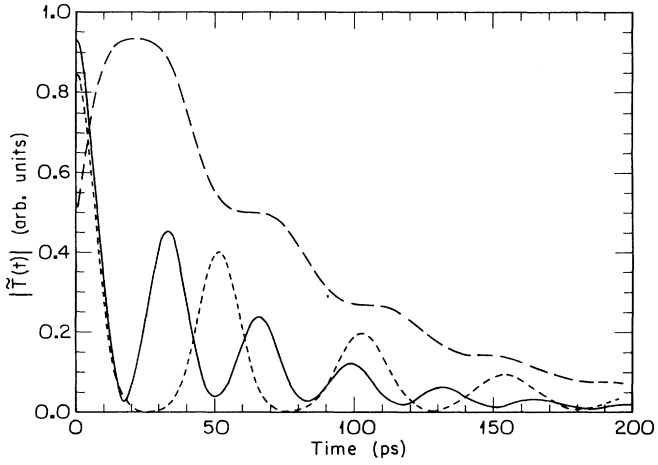

FIG. 3. Three time profiles, calculated using 10-ps laser pulses. The short-dashed line represents the dipole magnitude when the laser is on line center. The solid line represents the dipole magnitude enhanced by a factor of 14, when the laser is tuned five states to the red. The long-dashed line represents the dipole magnitude enhanced by a factor of 10, when the laser is tuned five states to the blue.

of the Rydberg electron, but rather an excitation of the ion core, near its resonance transition. Consequently, very little laser power is required to make these transitions, and it will even be possible to saturate such a transition with current lasers. For example, the $6s \rightarrow 6p_{3/2}$ barium-ion transition can be saturated in 10 ps with a laser power of 10 MW/cm^2 [11], in contrast to the powers of 400 MW/cm^2 or 3.5 GW/cm^2 used in the one-electron experiments [7]. Such a low laser power corresponds to a laser fluence of only 0.1 mJ/cm^2. Consequently, it should be possible to excite the core electron with a π pulse [14] to achieve complete inversion, and then to measure the dipole-moment evolution by deexciting with a second, delayed π pulse.

However, π pulsing the core is not the only way to study the core-dipole-moment evolution, because the alkaline earth ions have an entire series of alkalilike transitions. Consequently, the core electron can be further excited to produce yet a higher doubly excited state [15], as long as its incident dipole moment is intact. Several groups have already studied the $7snl$ states of barium by using two-photon, stepwise excitation to drive transitions such as $6snl \rightarrow 6pnl \rightarrow 7snl$ [16]. Typically, the two-photon excitations are detected by analyzing the energy spectra of the electrons ejected by autoionization, after the two-photon core transition is completed, to separate the one-photon and two-photon ionization processes. The second step of this excitation also requires relatively low laser power, since the $6p \rightarrow 7s$ transition moment is approximately half as large as that for the $6s \rightarrow 6p$ transition.

In conclusion, we have shown that two-electron-like atoms can be excited to wave-packet states showing classical behavior in their core-dipole-moment *decay,* which changes at specific times separated by the Rydberg orbit period. This discretizes the decay process, showing another example of how a fundamental quantum system can naturally evolve into classical time behavior. These two-electron-like atoms can also show wave-packet behavior similar to that of one-electron-like atoms when off-resonance excitation is used. With these two-electron-like Rydberg wave-packet states, excitation *and* detection will be easier, opening several new avenues for time-resolved atomic state studies.

This work was supported by the National Science Foundation under Grant No. PHY88-14903.

[1] J. Parker and C. R. Stroud, Jr., Phys. Rev. Lett. **56**, 716 (1986).

[2] G. Alber, H. Ritsch, and P. Zoller, Phys. Rev. A **34**, 1058 (1986).

[3] A. ten Wolde, L. D. Noordam, H. G. Muller, A. Lagendijk, and H. B. van Linden van den Heuvell, Phys. Rev. Lett. **61**, 2099 (1988).

[4] W. A. Henle, H. Ritsch, and P. Zoller, Phys. Rev. A **36**, 683 (1987).

[5] M. Prelomov, Commun. Math. Phys. **26**, 222 (1972); M. M. Nieto and L. M. Simmons, Jr., Phys. Rev. D **20**, 1321 (1979).

[6] J. Parker, C. R. Stroud, Jr., Phys. Scr. **T12**, 70 (1986).

[7] J. A. Yeazell, M. Mallalieu, and C. R. Stroud, Jr., Phys. Rev. Lett. **64**, 2007 (1990).

[8] J. A. Yeazell and C. R. Stroud, Jr., Phys. Rev. A **35**, 2806 (1987); Phys. Rev. Lett. **60**, 1494 (1988).

[9] W. E. Cooke, T. F. Gallagher, S. A. Edelstein, and R. M. Hill, Phys. Rev. Lett. **41**, 178 (1978).

[10] W. E. Cooke and C. L. Cromer, Phys. Rev. A **32**, 2735 (1985); N. H. Tran, P. Pillet, R. Kachru, and T. F. Gallagher, Phys. Rev. A **29**, 2640 (1984).

[11] S. A. Bhatti, C. L. Cromer, and W. E. Cooke, Phys. Rev. A **24**, 161 (1981).

[12] S. M. Jaffe, R. Kachru, H. B. van Linden van den Heuvell, and T. F. Gallagher, Phys. Rev. A **32**, 1480 (1985).

[13] P. Camus, M. Dieulin, and A. El Himdy, Phys. Rev. A **26**, 379 (1982).

[14] Charles P. Slichter, in *Principles of Magnetic Resonance* (Harper Row, New York, 1963), p. 20.

[15] J. Boulmer, P. Camus, J. M. Lecomte, and P. Pillet, J. Opt. Soc. Am. B **5**, 2199 (1988); U. Eichmann, V. Lange, and W. Sander, Phys. Rev. Lett. **64**, 274 (1990).

[16] T. F. Gallagher, R. Kachru, N. H. Tran, and H. B. van Linden van den Heuvell, Phys. Rev. Lett. **51**, 1753 (1983); R. P. Jopson, R. R. Freeman, W. E. Cooke, and J. Bokor, Phys. Rev. A **29**, 3154 (1984).